JOURNAL OF AIRCRAFT
Vol. 31, No. 4, July–Aug. 1994

Forebody Tangential Slot Blowing on an Aircraft Geometry

Ken Gee*
MCAT Institute, Moffett Field, California 94035
and
Yehia M. Rizk† and Lewis B. Schiff‡
NASA Ames Research Center, Moffett Field, California 94035

The effect of forebody tangential slot blowing on the flowfield about an F/A-18 aircraft is investigated numerically using solutions of the Navier-Stokes equations. Computed solutions are obtained for an aircraft geometry, which includes the fuselage, a wing with deflected leading-edge flap, empennage, and a faired-over engine inlet. The computational slot geometry corresponds to that used in full-scale wind-tunnel tests. Solutions are computed using flight test conditions and jet mass flow ratios equivalent to wind-tunnel test conditions. The effect of slot location is analyzed by computing two nontime-accurate solutions with a 16-in. slot located 3 in. and 11 in. aft of the nose of the aircraft. These computations resolve the trends observed in the full-scale wind-tunnel test data. The flow aft of the leading-edge extension vortex burst is unsteady. A time-accurate solution is obtained to investigate the flow characteristics aft of the vortex burst, including the effect of blowing on tail buffet.

Nomenclature

A_j = jet exit area
A_{ref} = wing reference area, 400 ft^2
a_∞ = freestream speed of sound, $\sqrt{\gamma RT_\infty}$
C_n = total aircraft yawing moment coefficient, $(M_y/q_\infty A_{ref}\bar{c})$
$C_{n,tail}$ = total yawing moment coefficient on vertical tail, $(M_{y,tail}/q_\infty A_{ref}\bar{c})$
C_y = total aircraft side force coefficient, $(Y/q_\infty A_{ref}\bar{c})$
$C_{y,tail}$ = total side force coefficient on vertical tail, $(Y_{tail}/q_\infty A_{ref}\bar{c})$
$\bar{c}$ = mean aerodynamic chord, 11.54 ft
c_n = local aircraft yawing moment coefficient, $(m_y/q_\infty A_{ref}\bar{c})$
c_{root} = wing root chord, 15.83 ft
dt = nondimensional time step
M_y = total aircraft yawing moment
$M_{y,tail}$ = total yawing moment on vertical tail
M_∞ = freestream Mach number, V_∞/a_∞
MFR = mass flow ratio, $(\rho_j V_j A_j/\rho_\infty V_\infty A_{ref})$
m_y = local aircraft yawing moment
q_∞ = freestream dynamic pressure, $\frac{1}{2}\rho_\infty V_\infty^2$
R = gas constant, air
$Re_{\bar{c}}$ = Reynold number based on mean aerodynamic chord, $(\rho_\infty V_\infty \bar{c}/\mu_\infty)$
T_∞ = freestream temperature
$\bar{t}$ = nondimensional time, $(ta_\infty/\bar{c})$
V_j = jet exit velocity
V_∞ = freestream velocity
Y_{tail} = total side force on vertical tail
α = angle of attack
γ = ratio of specific heats
ρ_j = jet exit density
ρ_∞ = freestream density

Presented as Paper 93-2962 at the AIAA 24th Fluid Dynamics, Plasmadynamics, and Lasers Conference, Orlando, FL, July 6–9, 1993; received July 26, 1993; revision received Nov. 29, 1993; accepted for publication Dec. 6, 1993.

*Research Scientist. Member AIAA.
†Research Scientist. Associate Fellow AIAA.
‡Special Assistant for High Alpha Technology. Associate Fellow AIAA.

Introduction

EXPANDING the high-angle-of-attack capabilities of combat aircraft, typified by the F/A-18 HARV, has been a focus of research in recent years. However, the complex nature of the flowfield in the high-alpha flight regime presents challenges in developing methods for enhanced aerodynamic control. As the angle of attack increases, the vertical tails become immersed in the low-energy, separated flow of the wings and fuselage, leading to a loss of directional control power. The high-alpha flowfield is dominated by vortices shed from the forebody and the wing leading-edge extensions (LEX). The forebody vortices may become asymmetrical, which can cause an uncontrolled departure of the aircraft from its intended flight path. Also, the LEX vortices can burst, leading to tail buffet on the twin vertical tails. Expanding the high-angle-of-attack flight envelope requires an understanding of these flow phenomena, and a means of providing the necessary control power.

One means of providing the necessary aerodynamic control power is to manipulate the forebody vortices using pneumatic forebody flow control. Two methods of pneumatic forebody flow control have been studied extensively over the past several years. One method is to use discrete jets located near the nose of the aircraft, blowing aft or inboard at some angle. Such jets have been studied for use on the F-16,[1] F/A-18,[2,3] and the X-29.[4] Use of discrete jets on the X-29 has proven to be quite effective in flight tests. The second pneumatic flow control method is tangential slot blowing. In this concept, a slot is located near the nose of the aircraft from which a thin sheet of air is ejected tangential to the surface of the body. The sheet remains attached to the surface for some circumferential distance past the no-blowing separation location before eventually separating, thus altering the forebody flowfield and creating a side force and yawing moment on the aircraft. Tangential slot blowing has been studied for use on the F-16[1] and F/A-18.[2]

Both experimental and computational data have been obtained for the F/A-18 with tangential slot blowing. Subscale water-tunnel tests[2,5] indicated that the method is a viable means of generating yawing moment. Isolated forebody compu-

tations[6,7] showed that the method worked at flight test conditions. Analogous to the results reported by Degani[8,9] in investigations of flows over an ogive-cylinder with small geometric perturbations located near the tip, a slot located nearest the tip of the nose of the aircraft was found to be the most efficient in the isolated forebody computations.[6] These computed results guided development of a baseline slot geometry tested in the Ames 80- by 120-ft wind tunnel.[3] The full-scale wind-tunnel test[3] provided experimental data at full-scale Reynolds numbers. In addition, computations carried out for the wind-tunnel test conditions were compared with measured data to validate the computational method.[10]

This article presents additional numerical analysis of the pneumatic slot blowing concept. An objective of the work is to extrapolate the measured wind-tunnel trends to actual aircraft flight conditions using the aircraft geometry, instead of the isolated forebody geometry. Non-time-accurate aircraft solutions are presented for two slot geometries and compared with experimental data. The computed results confirm the trends found experimentally at high Reynolds number. Furthermore, it is found that the interaction between the fuselage flowfield and flow over the aft end of the aircraft can have significant effects on the loading of the vertical tails. To investigate these effects, time-accurate solutions of the unsteady flowfield due to blowing are presented, and compared with previous time-accurate, no-blowing computational results.

Computational Method

Governing Equations and Flow Solver

At large angles of attack, the flow around an aircraft is characterized by large regions of three-dimensional separated flows and concentrated vortices above the aircraft. As a result, the Reynolds-averaged, thin-layer Navier-Stokes equations are solved to obtain the relevant flow features. These equations are solved numerically using the F3D[11] code. F3D is a two-factor, implicit, finite-difference algorithm with an approximately factored, partially flux-split scheme. The F3D code has proven to be accurate and reliable in solving such high-angle-of-attack problems as the steady flowfield about bodies of revolution[12] and the F-18 forebody,[13] and unsteady flowfields about the full F-18 configuration.[14] Non-time-accurate computations are an efficient method of obtaining a mean flowfield about the F/A-18. To determine the physical details in the unsteady portion of the flow, time-accurate solutions are required, even though such solutions require more computational effort. A full description of the flow solver may be found in Refs. 11, 12, and 14.

Closure of the Navier-Stokes equations is obtained using an algebraic eddy-viscosity turbulence model. In the present work, the Baldwin-Lomax algebraic model[15] is used throughout the flowfield except in the regions of the forebody, the boundary-layer diverter, and in the region between the wing flap and the fuselage. In the forebody region, the Baldwin-Lomax model with the high-alpha modifications due to Degani and Schiff[16] is used. In the boundary-layer diverter region, and in the region between the wing flap and the fuselage, a simplified model using only the inner-layer equation from the the Baldwin-Lomax model is used. Since only the gross effects of viscosity on the flow in these regions is necessary, the use of this simplified model has proven to be adequate.[14]

Computational Grid

The full F-18 overset/patch grid geometry is shown in Fig. 1. It is comprised of 20 grids containing a total of 1.8 million grid points. An analogous 10-grid model was used in previous full-body, zero-sideslip computations, which gave good results when compared with flight-test data.[14] The current grid system is obtained by reflecting the 10-grid system about the symmetry plane. As seen in Fig. 1, the wing leading-edge flaps are deflected 33-deg nose down, the trailing-edge flaps are undeflected, and the horizontal tails are deflected 7-deg nose down. The deflection angles of these control surfaces correspond to the trim flight condition of the F-18 at 30-deg angle of attack. The major features of the aircraft are well represented. However, several simplifications to the geometry are made to facilitate mathematical modeling. In particular, the engine inlets are faired over with no flow through the fairing, and the boundary-layer diverter grid is highly simplified.

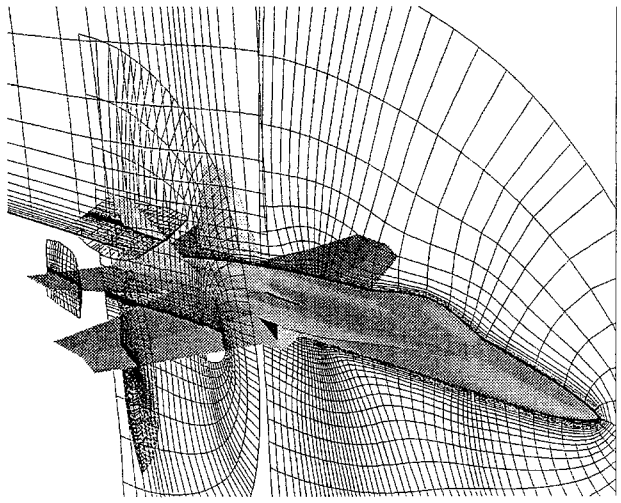

Fig. 1 Grids modeling F-18 geometry.

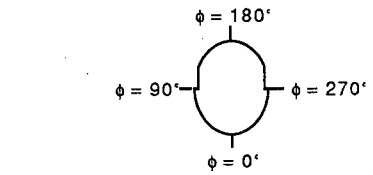

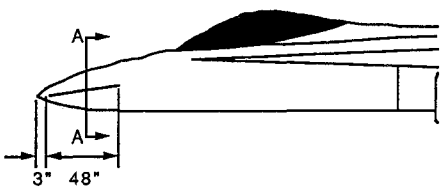

Fig. 2 Schematic of slot configuration.

The forebody blowing slot geometry (Fig. 2) is modeled using two additional grids. Slots are included on both sides of the body to match the full-scale experimental configuration, although blowing occurs only from the port slot. The length of the experimental slot is 48 in., and is composed of sections attached to separate plenums such that the length of the tangential jet can be controlled. In the computational grid, the total length of the slot is modeled, and the active jet region is modeled through the use of appropriate boundary conditions. This is done to account for the effects of the backward-facing step of the slot geometry on the flowfield characteristics.[7] The slot grids extend from the slot location to the leeward plane of symmetry and from the surface into the far field. This simplifies the implementation of an algebraic turbulence model in the slot region.

Slot Boundary Conditions

The current computations utilize jet boundary conditions reported in Ref. 10. The jet exit Mach number and the jet mass flow rate are obtained by matching the jet MFR with the full-scale experimental data. The jet exit pressure is assumed to be the local pressure value at a point just above the slot, in the direction normal to the body surface. This exit pressure is updated at each iteration step. The density of the jet is computed from the known mass flow rate, jet exit Mach number, and the measured plenum temperature.

Results and Discussion

One objective of this study is to extrapolate the experimental results measured in the full-scale wind-tunnel test to actual flight-test conditions using the aircraft grid model. Thus, solutions for the aircraft geometry are obtained using two slot geometries. One geometry consists of an active slot length of 16 in. beginning 3 in. aft of the nose of the F/A-18 (hereafter referred to as the 16–3-in. slot). The other geometry consists of a 16-in.-long active slot beginning 11 in. aft of the nose (16–11-in-slot). The solutions are obtained at a flight condition of $M_\infty = 0.243$, $a = 30.3$ deg, and $Re_{\bar{c}} = 11.0 \times 10^6$. The jet conditions are set such that the MFR $= 1.27 \times 10^{-4}$, matching an MFR of the wind-tunnel experiment. Blowing is from the port side; therefore, the side force and yawing moment produced by blowing is directed to port and is therefore negative.

Initially, non-time-accurate solutions are obtained using both slot configurations. Non-time-accurate solutions require less computational time since the time step may be increased and the convergence rate decreased. However, if the flowfield is unsteady, the solutions will not converge, but rather exhibit a nonphysical unsteadiness. When this behavior is observed, a time-accurate solution is obtained, starting from the non-time-accurate solution, to more accurately resolve the unsteadiness in the flowfield. For this study, a time-accurate solution is obtained using the 16–11-in. slot.

Flowfield Characteristics

Both the non-time-accurate and time-accurate solutions indicate the flowfield forward of the LEX vortex burst points to be steady, and both types of solutions resolve the essential characteristics of the flowfield. Off-surface instantaneous streamlines obtained from the non-time-accurate solutions (Fig. 3) indicate that the flowing-side LEX vortex bursts forward of the nonblowing-side LEX vortex. This is consistent with flow visualizations obtained in the full-scale wind-tunnel tests.[17] However, the computed burst point locations are aft of the burst point locations observed experimentally. This is due to the relatively coarse grid used in these computations, which has been shown to have an effect on the burst point location.[18] The vertical tails are immersed in the flow aft of the LEX vortex bursts.

On the forebody, where the flow is steady, the computed surface flow pattern shown in Fig. 4 indicates the separation line due to the jet from the 16–3-in. slot (Fig. 4a) to be closer to the leeward plane of symmetry than the separation line due to the jet from the 16–11-in. slot (Fig. 4b). Aft of the slot region, a separation line forms on the forebody. This separation line is longer in the case of the 16–3-in. slot, since the slot is located further forward on the nose.

The helicity density contours[19] at fuselage station 327, shown in Fig. 5, shows the asymmetry in the LEX vortices caused by blowing. Fuselage station 327 is forward of the blowing-side computed vortex burst point. The blowing-side LEX vortex appears to be relatively stronger than the non-blowing-side LEX vortex, leading to the asymmetric burst point positions observed in Fig. 3. The helicity density contours from the isolated forebody solutions also indicate this difference in vortex strength.[6] Similar changes in the strengths of the blowing- and non-blowing-side vortices, caused by tangential slot blowing, is observed in computed solutions involving an ogive-cylinder.[20,21] Indeed, Font[21] uses this behavior to identify force production mechanisms in tangential slot blowing. Comparing the two non-time-accurate aircraft solutions, the 16–3-in. slot case (Fig. 5a) has a blowing-side LEX vortex that is slightly stronger than the blowing-side LEX vortex in the 16–11-in. slot case (Fig. 5b). However, the non-blowing-side LEX vortex in the 16–3-in. slot case is also stronger than the corresponding non-blowing-side vortex in the 16–11-in. slot solution.

Yawing Moment Distribution

The local yawing moment distribution along the aircraft length for both non-time-accurate solutions are presented in Fig. 6. The local yawing moment is defined as the local sectional side force multiplied by the distance from the section to the moment center (fixed at fuselage station 454). The 16–11-in. slot generates a slightly greater local yawing moment

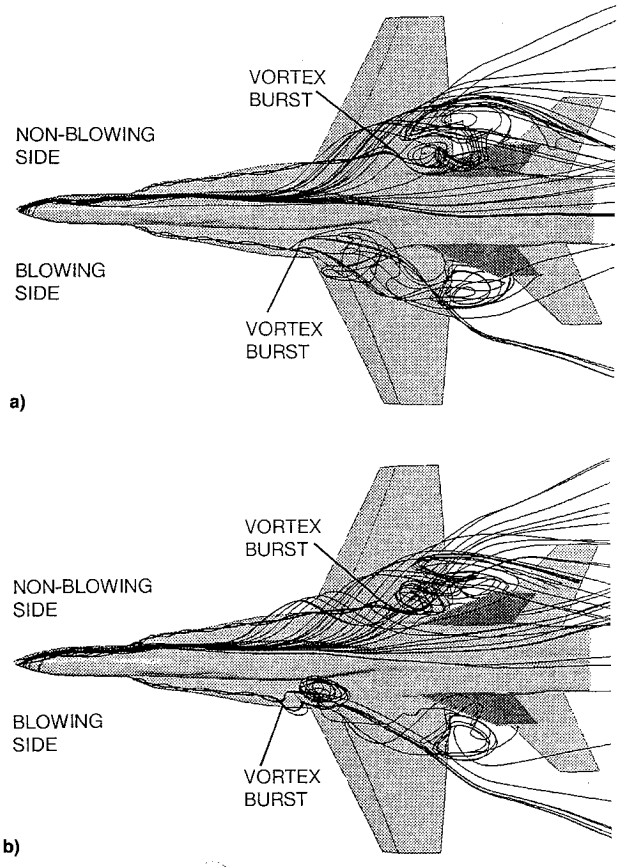

Fig. 3 Computed off-surface instantaneous streamlines. $M_\infty = 0.243$, $\alpha = 30.3$ deg, $Re_{\bar{c}} = 11.0 \times 10^6$, MFR $= 1.27 \times 10^{-4}$: a) 16–3-in. slot and b) 16–11-in. slot.

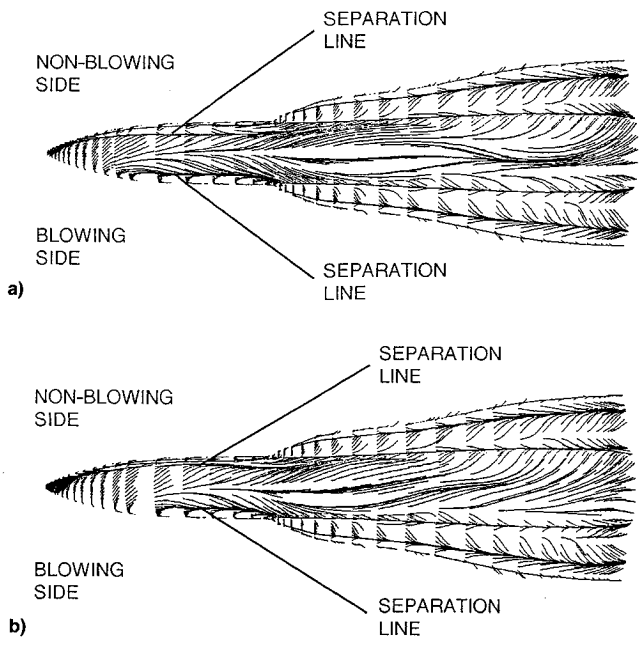

Fig. 4 Computed surface flow pattern on forebody. $M_\infty = 0.243$, $\alpha = 30.3$ deg, $Re_{\bar{c}} = 11.0 \times 10^6$, MFR $= 1.27 \times 10^{-4}$: a) 16–3-in. slot and b) 16–11-in. slot.

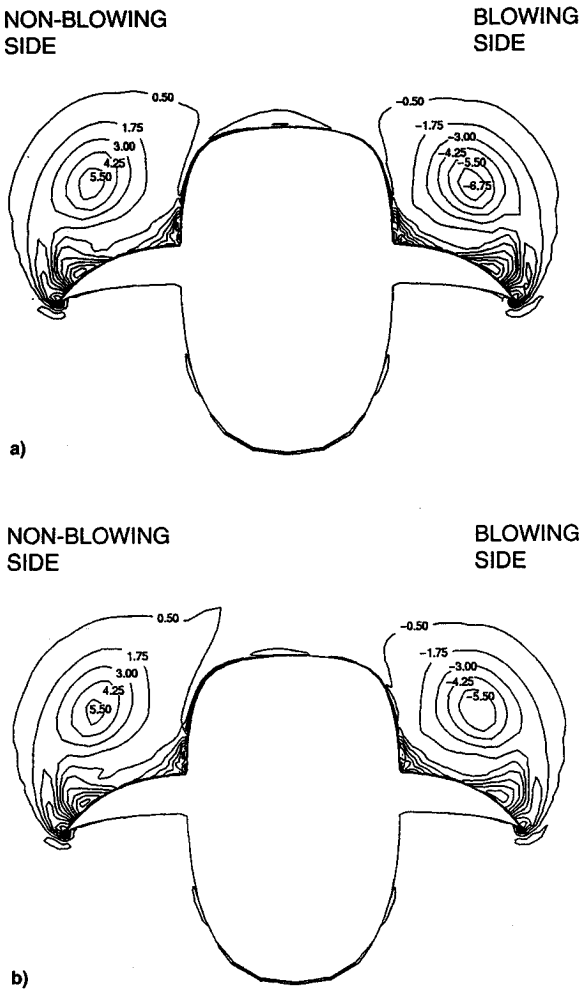

Fig. 5 Computed helicity density contours at fuselage station 327. $M_\infty = 0.243$, $\alpha = 30.3$ deg, $Re_c = 11.0 \times 10^6$, MFR = 1.27×10^{-4}: a) 16–3-in. slot and b) 16–11-in. slot.

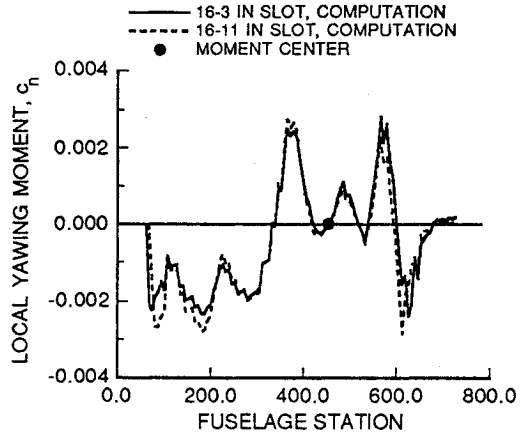

Fig. 6 Computed local yawing moment distribution. $M_\infty = 0.243$, $\alpha = 30.3$ deg, $Re_c = 11.0 \times 10^6$, MFR $= 1.27 \times 10^{-4}$.

than the 16–3-in. slot in the vicinity of the active slot, up to fuselage station 100. Since the radius of the forebody is greater in the region of the 16–11-in. slot, the jet creates a larger area of low pressure, leading to a greater local side force and yawing moment. In both cases, a yawing moment is produced in the region of the forebody forward of the blowing-side LEX vortex burst location, between fuselage station 100 and 350, due to the difference in the strengths of the forebody and LEX vortices. The 16–11-in. slot solution shows a larger local yawing moment than the 16–3-in. slot solution in this region. This indicates the difference in vortex strength is greater in the 16–11-in. slot case, even though the 16–3-in. slot case has a relatively stronger blowing-side LEX vortex (Fig. 5).

Although the flowfield is unsteady aft of the vortex burst (F. S. 350), the yawing moment distribution does show, qualitatively, the effects of the asymmetric burst point locations. The blowing-side aurface pressure increases aft of the blowing-side LEX vortex burst; therefore, the local yawing moment becomes positive due to the low pressure produced by the still-coherent non-blowing-side LEX vortex. There is also a local yawing moment in the region of the vertical tails, aft of fuselage station 525. The 16–11-in. slot solution shows a slightly more negative yawing moment in this region.

The computed local yawing moment distribution (Fig. 6) indicates that a large contribution to the total yawing moment occurs aft of the slot location. This is also evident in the blowing experiments involving the F-16[1] and the X-29.[4] The X-29 test[4] uses both a full aircraft and isolated forebody model, and the c.p. location is quite different for the two models. It appears that although isolated forebody computations can accurately resolve the local flow features such as surface pressure,[10] full aircraft configuration computations are required to determine the full effect of blowing on force and moment generation.

Time-Accurate Yawing Moment Analysis

To resolve the unsteadiness in the flowfield, a time-accurate solution is obtained using the 16–11-in. slot. The time-accurate solution is started from the non-time-accurate solution when the oscillatory nature of the total yawing moment is first observed. The time-accurate solution is computed using rigid vertical tails. A constant time step of $dt = 0.0025$ is used, which is determined by code numerical stability considerations. This time step is nondimensionalized using c_{root} and a_∞.

The time history of the total aircraft yawing moment is presented in Fig. 7. The yawing moment is oscillatory in nature. After an initial transient, the unsteadiness reduces to oscillations about the mean value of the yawing moment. It was found that the non-time-accurate solution, after the onset of the nonphysical unsteadiness in the solution, yielded total aircraft yawing moment values that fell within the range of values obtained in the time-accurate case. This indicates that the averaged value obtained from the nontime-accurate solutions should approximate the value obtained from the time-accurate solution.

In the wind-tunnel test,[3] it was found that a reduced tunnel velocity ($M_\infty = 0.115$, $q_\infty = 20$ psf), the 16–11-in. slot was more effective than the 16–3-in. slot. However, at maximum tunnel velocity ($M_\infty = 0.15$, $q_\infty = 33$ psf), both the 16–3-in. and 16–11-in. slots generated the same yawing moment coefficient for the same mass flow ratios. The numerical results, obtained at higher velocity flight-test conditions ($M_\infty = 0.243$. $q_\infty = 33$ psf), confirm the $M_\infty = 0.15$ wind-tunnel trends. A comparison of the computed total aircraft yawing moment

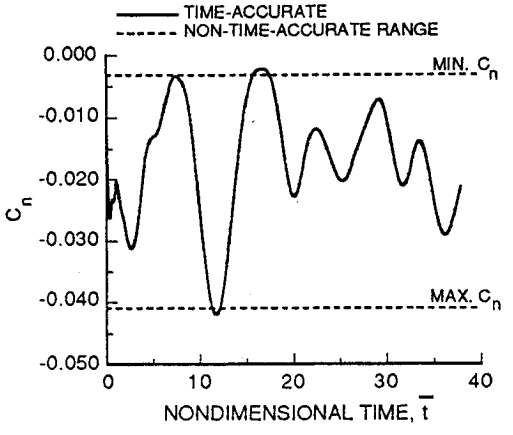

Fig. 7 Computed time history of total yawing moment.

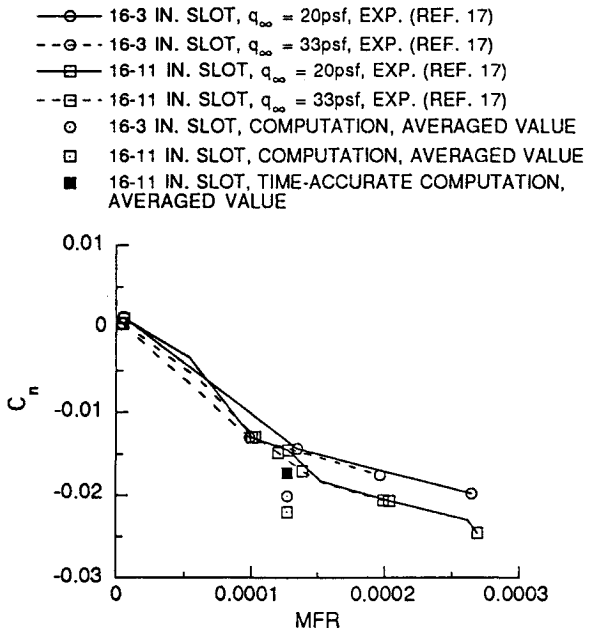

Fig. 8 Comparison of total yawing moment.

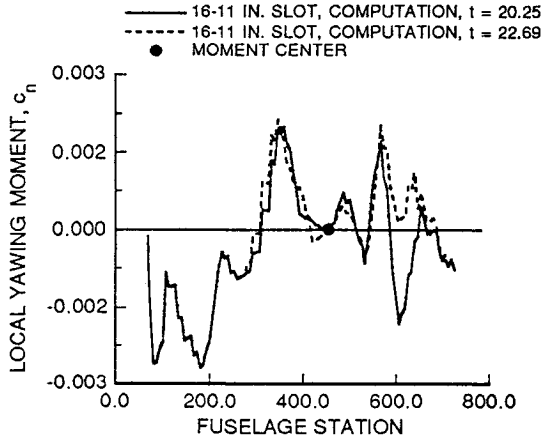

Fig. 9 Computed local yawing moment distribution at two points in time history.

with the full-scale wind-tunnel data,[3] shown in Fig. 8, indicates that the 16–11-in. slot generates essentially the same yawing moment coefficient as the 16–3-in. slot for a given mass flow ratio, and both solutions agree fairly well with the full-scale data. Both non-time-accurate yawing moment coefficients are somewhat higher than those measured in the experiment, but this may be due in part to the inability of the non-time-accurate solutions to accurately resolve the unsteadiness in the flow. The time-averaged yawing moment coefficient, obtained from the time-accurate solution, is in better agreement with the experimental data. The slight discrepancy may be attributed to the difference in the LEX vortex burst point locations between the computation and experiment. These results support the notion that the mass flow ratio is a good correlation factor for tangential slot blowing.

Effect of Vertical Tails on Aircraft Yawing Moment

Figure 9 presents the local yawing moment distribution along the body for two instants in time, one taken at a local maximum yawing moment point ($\bar{t}$ = 20.25 in Fig. 7), and the other taken at a local mimimum yawing moment point ($\bar{t}$= 22.69 in Fig. 7). The effect of the vertical tails on the total yawing moment is evident in this figure. The flow over the forebody and LEX region forward of the blowing-side LEX vortex burst is essentially steady, since the local yawing moment does not change with time. There is, however, a large difference in the local yawing moment in the vertical tail region. At $\bar{t}$ = 20.25, the vertical tails generate a negative yawing moment, thus increasing the total yawing moment. At $\bar{t}$ = 22.69, the vertical tails generate a positive yawing moment, thus reducing the total yawing moment produced by blowing. In the X-29 wind-tunnel experiment,[4] the single vertical tail was shown to have an influence on the side force and yawing moment, although at 30-deg angle of attack, the influence was minor. However, in the case of the F/A-18, with the twin vertical tails fully immersed in the unsteady flow aft of the LEX vortex bursts, the effect of the vertical tails is expected to be larger.

Analysis of Vertical Tail Aerodynamic Loads

The time history of the side force on the vertical tails is presented in Fig. 10. Since the tails are aft of the moment center, a positive side force on either tail generates a negative contribution to the total aircraft yawing moment. In Fig. 10, the positive side force on the blowing-side (port) tail increases the total aircraft yawing moment, while the negative side force on the nonblowing-side (starboard) tail decreases the total aircraft yawing moment. The fluctuations in the tail loading, in turn, leads to the change in local yawing moment in the vertical tail region observed in Fig. 9.

The bending moments applied to the vertical tails due to the aerodynamic forces are computed and presented in Fig. 11. The bending moment center is taken to be the root of the vertical tail. A fast Fourier transform analysis is performed on this data (Fig. 12) using 8192 steps. The fast Fourier transform shows a frequency peak in the blowing-side tail bending moment loads at 9 Hz. The bending moment applied to the non-blowing-side vertical tail has a dominant frequency at 12 Hz. Compared to the frequency obtained in previous computations about the F-18 geometry without blowing[14,22] and various experiments[23–25] (Fig. 13), it appears that blowing decreases the dominant frequency of the airloads slightly, thus

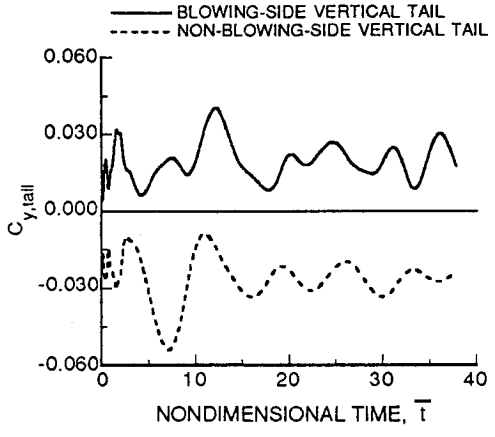

Fig. 10 Comparison of computed vertical tail side force time histories.

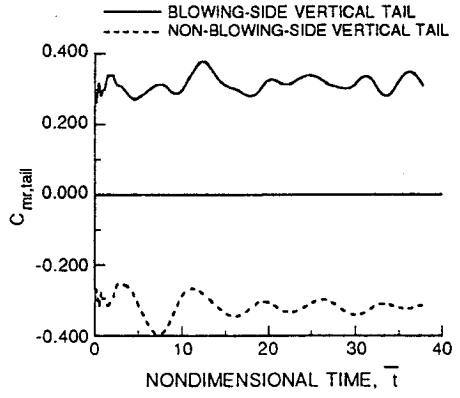

Fig. 11 Comparison of computed vertical tail bending moment time histories.

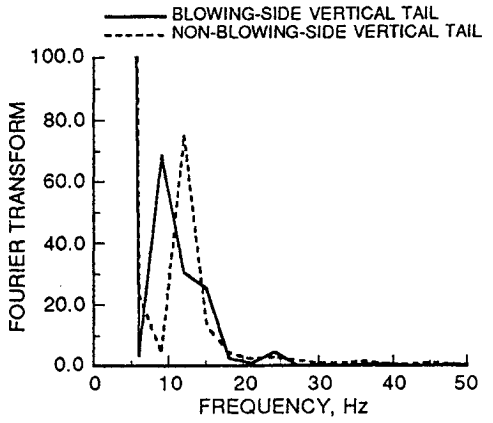

Fig. 12 Fast Fourier transform of computed vertical tail bending moment time histories.

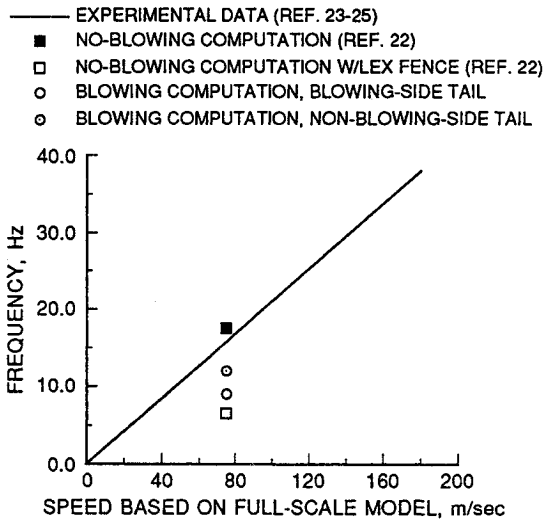

Fig. 13 Computed dominant frequencies in flowfield and experimental tail buffet frequency data.

moving away from the first bending natural frequency of the vertical tails, which was found to be about 15 Hz.[22] Since blowing affects the frequency content of the unsteady flow aft of the vortex burst, blowing has the potential to control tail buffet on the F-18 in a manner similar to that used on a rounded leading-edge delta wing.[26] In the delta wing case, symmetric tangential leading-edge slot blowing was used to reduce tail buffet by effectively changing the angle of attack of the wing.

Conclusions

The effect of slot location on the efficiency of forebody tangentail slot blowing on the F/A-18 was analyzed using two non-time-accurate, full aircraft computations. One slot geometry consisted of a 16-in. active slot located 3 in. from nose, whereas the other had a 16-in. active slot located 11 in. from the nose. Solutions were obtained using flight conditions and a mass flow ratio corresponding to a wind-tunnel experimental value. Blowing from the 16–11-in. slot generated slightly greater local yawing moment in the slot region and over the LEX than similar blowing from the 16–3-in. slot. However, the total aircraft yawing moment coefficient generated by both slots at flight-test conditions (and identical mass flow ratios) were essentially the same. This result confirms the trend found in the full-scale wind-tunnel data measured at maximum tunnel velocity.

The computations indicated a large interaction between the forebody and LEX flows and flow over the aft end of the aircraft. This showed the necessity of using full aircraft computations to predict the total yawing moment due to blowing, even though isolated forebody computations resolved the local forebody effects accurately.

The unsteadiness of the flow aft of the LEX vortex burst was analyzed by computing a time-accurate solution using the 16–11-in. slot geometry. The total yawing moment was found to be oscillatory and dependent on the local yawing moment contribution of the vertical tails. The average aircraft yawing moment agreed fairly well with experimental measurements. A fast Fourier transform analysis of the aerodynamic loads causing bending moment on the vertical tails yielded a dominant frequency slightly lower than that obtained from previous no-blowing computations, although the flow over the blowing-side vertical tail still contains a frequency peak within the natural frequency range of the vertical tails. This indicated that forebody tangential slot blowing had an effect on the frequency content of the flow, which in turn would affect tail buffet.

Acknowledgment

This work was partially funded by NASA Grant NCC 2-657.

References

[1]LeMay, S. P., Sewall, W. G., and Henderson, J. F., "Forebody Vortex Flow Control on the F-16C Using Tangential Slot and Jet Nozzle Blowing," AIAA Paper 92-0019, Jan. 1992.

[2]Ng, T. T., and Malcolm, G. N., "Aerodynamic Control Using Forebody Blowing and Suction," AIAA Paper 91-0619, Jan. 1991.

[3]Lanser, W. R., Meyn, L. A., and James, K. D., "Forebody Flow Control on a Full-Scale F/A-18 Aircraft," AIAA Paper 92-2674, June 1992.

[4]Guyton, R. W., and Maerki, G., "X-29 Forebody Jet Blowing," AIAA Paper 92-0017, Jan. 1992.

[5]Ng, T. T., Suarez, C. J., and Malcolm, G. N., "Forebody Vortex Control Using Slot Blowing," *AIAA 9th Applied Aerodynamics Conference* (Baltimore, MD), AIAA, Washington, DC, 1991, pp. 412–422 (AIAA Paper 91-3254).

[6]Gee, K., Tavella, D., and Schiff, L. B., "Computational Optimization of a Pneumatic Forebody Flow Control Concept," *AIAA 9th Applied Aerodynamics Conference* (Baltimore, MD), AIAA, Washington, DC, 1991, pp. 370–380 (AIAA Paper 91-3249).

[7]Murman, S. M., Rizk, Y. M., Cummings, R. M., and Schiff, L. B., "Computational Investigation of Slot Blowing for Fuselage Forebody Flow Control," AIAA Paper 92-0020, Jan. 1992.

[8]Degani, D., and Schiff, L. B., "Numerical Simulation of the Effect of Spatial Disturbances on Vortex Asymmetry," *AIAA Journal*, Vol. 29, No. 3, 1991, pp. 344–352.

[9]Degani, D., "Numerical Investigation of the Origin of Vortex Asymmetry," AIAA Paper 90-0593, Jan. 1990.

[10]Gee, K., Rizk, Y. M., Murman, S. M., Lanser, W. R., Meyn, L. A., and Schiff, L. B., "Analysis of a Pneumatic Forebody Flow Control Concept About a Full Aircraft Geometry," AIAA Paper 92-2678, June 1992.

[11]Steger, J. L., Ying, S. X., and Schiff, L. B., "A Partially Flux-Split Algorithm for Numerical Simulation of Compressible Inviscid and Viscous Flow," *Proceedings of a Workshop on Computational Fluid Dynamics*, Univ. of California, Davis, Davis, CA, 1986.

[12]Ying, S. X., Schiff, L. B., and Steger, J. L., "A Numerical Study of Three-Dimensional Separated Flow Past a Hemisphere Cylinder," AIAA Paper 87-1207, June 1987.

[13]Schiff, L. B., Cummings, R. M., Sorenson, R. L., and Rizk, Y. M., "Numerical Simulation of High-Incidence Flow over the F-18 Fuselage Forebody," AIAA Paper 89-0339, Jan. 1989.

[14]Rizk, Y. M., and Gee, K., "Unsteady Simulation of Viscous Flowfield Around F-18 Aircraft at Large Incidence," *Journal of Aircraft*, Vol. 29, No. 6, 1992, pp. 986–992.

[15]Baldwin, B., and Lomax, H., "Thin-Layer Approximation and Algebraic Model for Separated Turbulent Flows," AIAA Paper 78-0257, Jan. 1978.

[16]Degani, D., and Schiff, L. B., "Computation of Turbulent Supersonic Flows About Pointed Bodies Having Crossflow Separation," *Journal of Computational Physics*, Vol. 66, No. 1, 1986, pp. 173–196.

[17]Lanser, W. R., private communication, April 1992.

[18]Rizk, Y. M., Schiff, L. B., and Gee, K., "Numerical Simulation of the Viscous Flow Around a Simplified F/A-18 at High Angles of Attack," AIAA Paper 90-2999, Aug. 1990.

[19]Levy, Y., Degani, D., and Seginer, A., "Graphical Visualization

of Vortical Flows by Means of Helicity," *AIAA Journal*, Vol. 28, No. 8, 1990, pp. 1347–1352.

[20]Font, G. I., and Tavella, D. A., "High Alpha Aerodynamic Control by Tangential Fuselage Blowing," *AIAA Journal*, Vol. 30, No. 5, 1992, pp. 1321–1330.

[21]Font, G., "Force Production Mechanisms of a Tangential Jet on Bodies at High Alpha," AIAA Paper 92-4648, Aug. 1992.

[22]Rizk, Y., Guruswamy, G., and Gee, K., "Numerical Investigation of Tail Buffet on F-18 Aircraft," AIAA Paper 92-2673, June 1992.

[23]Martin, C. A., and Thompson, D. H., "Scale Model Measurements of Fin Buffet Due to Vortex Bursting on F/A-18," AGARD Fluid Dynamics Specialists Meeting, Paper 12, 1991.

[24]Meyn, L. N., and Ross, J. C., private communication, 1991.

[25]Del Frate, J. H., Freudinger, L. C., and Kehoe, M. W., "F-18 Tail Buffet," High Alpha Technology Program Workshop, Dryden Flight Research Center, Edwards, CA, 1989.

[26]Bean, D. E., and Wood, N. J., "An Experimental Investigation of Twin Fin Buffeting and Suppression," AIAA Paper 93-0054, Jan. 1993.